

# *IET Generation, Transmission & Distribution*

## Special issue Call for Papers

---

**Be Seen. Be Cited.  
Submit your work to a new  
IET special issue**



Connect with researchers and experts in your field and share knowledge.

Be part of the latest research trends, faster.

**Read more**



# A privacy-preserving approach to day-ahead TSO-DSO coordinated stochastic scheduling for energy and reserve

Mahdi Habibi  | Vahid Vahidinasab  | Mohammad Sadegh Sepasian

Faculty of Electrical Engineering, Shahid Beheshti University, Tehran 1983969411, Iran

## Correspondence

Vahid Vahidinasab, Faculty of Electrical Engineering, Shahid Beheshti University, Tehran, 1983969411, Iran.

Email: vahid.vahidinasab@iecc.org

## Abstract

Proliferation of distributed energy resources (DERs) calls for a coordinated transmission and distribution (T&D) scheduling at the day-ahead stage. The problem becomes more complicated dealing with the variability of stochastic parameters. Also, privacy and complexity are two barriers to the development of such coordinated platforms. This paper addresses these issues by introducing a hybrid centrally-supported decentralized stochastic framework for the day-ahead energy and reserve market with minimum complexity and the need for data-sharing between system operators. The proposed model is able to calculate the bidirectional power exchange at the T&D interface and the separated costs, dispatches, and reserves of all market participants. The proposed model does not consider any priority for operators and increases the liquidity by facilitating participants' access to the market platform. Also, the second-order cone programming (SOCP) formulation is used for calculating the AC power flow of distribution grids, and the model is validated and compared with other implementation strategies. The proposed model is implemented on a modified IEEE 24-bus test system, and results show that the model can schedule resources for supplying energy and reserves in both transmission and distribution levels in an acceptable computation time.

## 1 | INTRODUCTION

The active role of distribution system operators (DSOs) is highlighted with increasing renewable energy resources (RES) installed at the distribution grids and uncertainties dealing with the system operation at the day-ahead stage [1–3]. The use of distributed energy resources (DERs) by DSOs for local applications and congestion management or balancing by the transmission system operator (TSO) should be coordinated by a proper strategy to enhance economic performance and to prevent any interruptions [4]. This strategy should consider distribution grid constraints while violations of voltage constraints and lines' thermal limits jeopardize the economy and security of the operation. However, DSOs are reluctant to share detailed operational data [5, 6]. This paper develops a stochastic platform for the collaborative scheduling of energy and reserve for TSO and DSOs with the minimum complexity and operators' data-sharing.

### 1.1 | Literature survey

The NTSO-E and CEER reports emphasize that the system operators (SOs) should prepare a level play-field for all parties to access the market platform [7, 8]. So, neutrality and liquidity are two important features in developing platforms for coordinated energy markets [9]. Reference [10] analyzes four pioneering market implementing projects considering TSO-DSO cooperation. The assessment of TSO-DSO interactions developing in 9 countries is conducted in [11], where DERs are used for relieving congestion of the transmission and distribution (T&D) interface, congestion of transmission lines, balancing, and voltage support. Reference [12] compares conventional grid architecture with the new one with interactions between SOs and different new actors of the active distribution networks (ADN).

Different schemes are suggested for TSO-DSO coordination in the literature that can be classified into centralized,

This is an open access article under the terms of the [Creative Commons Attribution](https://creativecommons.org/licenses/by/4.0/) License, which permits use, distribution and reproduction in any medium, provided the original work is properly cited.

© 2021 The Authors. *IET Generation, Transmission & Distribution* published by John Wiley & Sons Ltd on behalf of The Institution of Engineering and Technology

decentralized, and hybrid types [13]. Reference [14] presents a centralized TSO-DSO dispatch considering mobile energy storage systems transferring between energy systems. The centralized models are straightforward and usually lead to the most optimal solutions. But, they have two significant drawbacks: (i) the unified model of T&D becomes very complex, (ii) sharing information between SOs is a big deal for this approach [5]. The privacy restrictions are issued in the grid topology, technical constraints, bid information etc. On the other hand, decentralized schemes can address privacy issues; however, the optimality and technical constraints must be preserved by solutions. In this regard, [15] and [16] determine P-Q flexibility maps at the T&D interface using a decentralized prequalification platform. However, that method only guarantees feasible service procurement, and the economic aspect of the solution has not been incorporated. The qualification procedures for resources located at the distribution level can be assigned to DSOs. The INTERFACE project evaluates the qualification procedures, including grid prequalification for accepting bids submitted by DERs, product prequalification based on specification and type of services, and bid qualification (market phase) [5]. Reference [17] considers a decentralized bid prequalification process based on the traffic light concept. However, the boundaries operation points are only evaluated for T&D power flow, and re-dispatches with additional cost may be needed. The hybrid frameworks use the advantages of both centralized and decentralized strategies [13]. Reference [18] calculates several 24-h power profiles at T&D interfaces and the prices to be used by the TSO for centralized dispatching. That hybrid method only considers reserves for potential projection of load and the output of RES in a deterministic model but does not lead to the optimal solution.

The decentralized and hybrid coordination schemes employ distributed optimization methods for scheduling T&D networks, which these methods can be classified into three categories: (i) the methods based on Lagrangian relaxation, including the alternating direction method of multipliers (ADMM) [19] and the analytical target cascading (ATC) method [20–22], (ii) optimality condition decomposition (OCD) methods such as heterogeneous decomposition methods [23–26], (iii) Benders decomposition methods [27, 28]. The coordination of T&D operators after major blackouts is investigated in [19], and the ADMM method is used to restore both networks by sharing limited information of border nodes within an iterative process. The optimal power flow optimization of TSO and DSOs is studied in [20] using the ATC method, in which the magnitude and angle of boundary buses are shared as intermediary variables. The execution time is not reported in that paper, but the algorithm convergence significantly depends on the estimated initial values for the decision variables. A distributed bi-level optimization based on parallelized ATC method is used in [21] for the unit commitment (UC) problem with the DC power flow formulation, in which the robustness of the solution against cyber-attacks and communication failures is investigated. Also, ref. [22] evaluates a decentralized framework for optimal scheduling of the independent system operator

and DSOs, in which the ATC method is used based on the concept of the system of systems. The market platform is fully decomposed in ATC methods, and the energy network will be managed by the own market operator and the corresponding cost function; however, the specification of energy piece at T&D interface would be an issue, especially if different SOs may calculate various locational marginal prices (LMPs) for the boundary nodes. As ref. [23] claimed, the complicated parameter setting process and the low convergence rate are other disadvantages of ATC methods.

The distributed optimization of T&D systems based on heterogeneous decomposition is described in [23]. In that study, the TSO calculates LMPs at boundary nodes, and ADNs calculate the amount of power injection to upstream networks. So, the proposed method of [23] is applicable for selling redundant capacity of distribution systems only in one direction to the TSO; however, in practice, a bidirectional power flow is expected between T&D networks. A similar basis is used in [24] and [25] to perform a multi-objective optimization and address the impact of communication delays on the convergence efficiency of the algorithm in the actual operation, respectively. Also, the distributed scheduling of the integrated heat and power energy systems is studied in [26] using heterogeneous optimization.

The Benders decomposition method is used in [27] for optimizing the reactive power for T&D networks and investigating the voltage problems and power loss; however, the deterministic model does not focus on market platform and optimal scheduling of energy or reserves. Reference [28] investigates optimal power flow of T&D systems to schedule energy and reserve using Benders decomposition. However, the deterministic case studied in that paper considers the outage of the largest generator as the criterion of supplying reserve capacities, and uncertainties are not evaluated. In addition, the model used in [27] and [28] investigates the optimal power flow problem at a snapshot of the system operation (not the UC problem at the day-ahead stage), and the share of market players is not calculated in that studies.

The active and reactive power flow of distribution networks are highly interdependent; hence, simultaneous control is needed [29]. A TSO-DSO coordination scheme for reactive power procurement from distribution networks, including wind farms, is proposed in [30], which does not optimize the active power trading between SOs. A local market for reactive power procured by DERs is presented by [31], and redundant values are submitted to be used by the TSO. The justification of second-order cone programming (SOCP) for AC power flow of ADNs is conducted in [32], and the accuracy of the model is compared to other methods.

Although the T&D interference more frequently appears in balancing and congestion management, involving DSOs in day-ahead scheduling will reduce the need for ancillary services in real-time operation [33]. The UC problem is usually applied for day-ahead scheduling of energy and reserves [34]. Reference [35] calculates LMPs of distribution networks in a centralized UC problem for T&D networks.

**TABLE 1** Taxonomy of existing publications in the field

Reference	Organization strategy	Power flow			Uncertainty handling features				Formulation (Solver)	Horizon of scheduling	Considered issues by the T&D coordination			
		Active	Reactive	BTDF <sup>a</sup>	RES	Load	Model	Reserve			PDS <sup>b</sup>	HMC <sup>c</sup>	OFS <sup>d</sup>	SSA <sup>e</sup>
[2]	Decentralized	✓	—	—	✓	—	Stochastic	✓	MILP	Day-ahead	—	—	—	—
[3]	Decentralized	✓	—	—	✓	—	Stochastic	✓	MILP	Day-ahead	—	—	—	—
[6]	Centralized	✓	—	—	—	—	Deterministic	—	MILP	Day-ahead	—	—	✓	—
[14]	Centralized	✓	—	✓	—	—	Deterministic	—	MILP	Day-ahead	—	—	✓	✓
[15]	Decentralized	✓	✓	—	—	—	Deterministic	✓	MINLP <sup>f</sup>	Real-time	✓	✓	—	—
[16, 17]	Decentralized	✓	✓	—	✓	✓	Deterministic	✓	MINLP	Real-time	✓	✓	—	—
[18]	Hybrid	✓	—	—	✓	✓	Deterministic	✓	MILP	Day-ahead	✓	✓	—	—
[20]	Decentralized	✓	✓	✓	—	—	Deterministic	—	NLP	Balancing	✓	—	—	—
[21]	Decentralized	✓	—	✓	—	—	Deterministic	—	MILP	Day-ahead	✓	—	—	—
[22]	Decentralized	✓	—	—	—	—	Deterministic	—	MISOCP	Day-ahead	✓	—	—	—
[23, 26]	Decentralized	✓	—	—	—	—	Deterministic	—	MILP/MINLP	Day-ahead	✓	✓	—	✓
[24, 25]	Decentralized	✓	✓	—	—	—	Deterministic	—	MINLP	Real-time	✓	✓	—	✓
[27, 28]	Hybrid	✓	✓	✓	—	—	Deterministic	—	SOCP	Balancing	✓	✓	—	—
[29]	Centralized	✓	✓	✓	—	—	Deterministic	—	MINLP	Real-time	—	—	—	—
[30]	Hybrid	—	✓	—	—	—	Deterministic	—	MINLP	Day-ahead	✓	✓	—	—
[31]	Decentralized	—	✓	—	—	—	Deterministic	—	MINLP	Real-time	✓	✓	—	✓
[34]	Decentralized	✓	—	—	✓	—	Stochastic	✓	MILP	Day-ahead	—	—	—	—
[35]	Decentralized	✓	✓	—	—	—	Deterministic	—	MINLP	Day-ahead	✓	—	—	✓
[36]	Decentralized	✓	—	—	✓	✓	Stochastic	✓	MILP	Day-ahead	—	—	—	—
This paper	Hybrid	✓	✓	✓	✓	✓	Stochastic	✓	MISOCP <sup>g</sup>	Day-ahead	✓	✓	✓	✓

<sup>a</sup>BTDF = Bidirectional T&D power flow.

<sup>b</sup>PDS = Privacy of data-sharing.

<sup>c</sup>HMC = Handling mathematical complexity.

<sup>d</sup>OFS = Optimality of feasible solutions.

<sup>e</sup>SSA = Specifying share of agents (precise amount and cost trading per SOs).

<sup>f</sup>MINLP = Mixed-integer non-linear programming.

<sup>g</sup>MISOCP = Mixed-integer SOCP.

## 1.2 | Research gaps

Table 1 classifies the existing publications developing the TSO-DSO coordination platforms, and features are compared with the presented model of this paper. Based on the literature review, the bidirectional energy trading between system operators, the calculation of fair values for the price of energy trading, and the incorporation uncertainties dealing with various networks are the gaps of previous studies. Hence, a platform is needed for scheduling energy and reserve in the day-ahead phase considering stochastic parameters and grid constraints for T&D systems with minimum data-sharing of SOs, in which a non-complex framework should specify the precise values of the operational costs for market participants and guarantee the liquidity and optimality of solutions.

## 1.3 | Contributions

This paper proposes a hybrid centrally-supported decentralized model for collaborative TSO-DSO stochastic scheduling of energy and reserve for the day-ahead market. The fluctuation of wind power generation and load forecasting errors at T&D systems are considered stochastic parameters. The Benders decomposition method was applied to solve the stochastic UC problem for the TSO in our previous studies [2, 3, 36]. This paper simultaneously reduces the complexity of the T&D integrated model and addresses the privacy issues by decomposing DSOs' level problems. As a result, the proposed platform requires minimum data exchange between SOs and incorporates the uncertainties associated with different SOs independently. The AC power flow is considered for distribution grids based on SOCP formulation, and the optimality of the feasible

solution is validated for both TSO and DSOs. The model employs a bidirectional power flow between T&D grids and calculates the exact share of SOs in the operational cost using LMPs. A modified IEEE 24-bus test system integrated with distribution grids is used to evaluate the performance and efficiency of the proposed model. The main specifications and the novel aspects of this paper are summarized as follows:

- The complexity of the TSO-DSO day-ahead stochastic scheduling is reduced by applying a decomposition method, while the constraints of distribution grids and the associated uncertainties are handled independently by individual system operators;
- The privacy issue is addressed by minimizing the need for data-sharing between market operators. The TSO and DSOs can directly, independently, and coordinately hold their markets to schedule energy and reserves optimally;
- The active and reactive power flow constraints are checked for DSOs using convex relaxation. Also, the calculated locational marginal prices at the transmission level reflect the cost of both the transmission and distribution systems. Hence, the precise charges of energy trading and the cost for every SOs are calculated using locational marginal prices and power exchange at boundary nodes of grids;
- The economic performance of the proposed framework is compared with other platforms, and the feasibility of the obtained decision variables for energy and reserve is validated based on network constraints.

## 1.4 | Organization of the paper

The rest of the paper is organized as follows. The proposed model of privacy-preserving TSO-DSO scheduling of energy and reserve is described in Section 2, and Section 3 evaluates results obtained by implementing the proposed platform on the test system. Finally, Section 4 concludes this paper.

## 2 | THE PRIVACY-PRESERVING MODEL TO DAY-AHEAD TSO-DSO COORDINATED STOCHASTIC SCHEDULING FOR ENERGY AND RESERVE

This section describes the model of the proposed stochastic privacy-preserving scheduling of TSO-DSO for the day-ahead energy market. The scenarios are considered to reflect the uncertainties in wind output and load forecasting errors. The original problem is decomposed into a master problem and two sub-problems using the Benders algorithm.

### 2.1 | Model of the TSO (master problem)

The master problem considers the TSO's grid constraints, while the sub-problems schedule the DSOs' level problem. In this

way, the TSO level problem is solved using intermediary variables without access to the downstream network's topology or any details of distributed generations. In the master problem, scenarios  $s \geq 1$  identify uncertainties at the transmission level, and  $s_0$  represents the base case scenario. The base case scenario obtains the basic schedule of the units to reflect the non-anticipativity constraint for the system operating point, and it will be used to ensure the feasibility of dispatches using the expected values of stochastic parameters. The objective function of the master problem is presented by Equation (1), and constraints are Equations (2)–(26). The objective function consists of the costs of energy and reserves supplied transmission level and the operating cost of DSOs. The energy cost includes charges to conventional generators (CGs), demand-side response (DSR) programs at the transmission level. Also, reserve costs incorporate the costs of reserve capacities in upward and downward directions provided by CGs, DSR programs, and wind farms. The auxiliary positive variable “ $\gamma_{D,t}$ ” incorporates lower bounds of DSOs' cost; hence, the objective cost function of the master problem considers the overall cost of T&D power systems.

$$\begin{aligned}
 \min_{\substack{p, \gamma, R, i, \\ dsr, st, sd}} \quad & \sum_{g,t} \left[ \sum_{j,s \geq 1} (\pi_{t,s} C_{j,g}^{En} p_{g,t}^{j,s}) \right. \\
 & \left. + C_g^{Fx} i_{g,t} + C_g^{ST} st_{g,t} + C_g^{SD} sd_{g,t} \right] \\
 & + \sum_{b,t} \sum_{s \geq 1} (\pi_{t,s} C_b^{En} dsr_{b,t}^s) + \sum_{g,t} (C_g^{Re,\uparrow} R_{g,t}^{\uparrow} + C_g^{Re,\downarrow} R_{g,t}^{\downarrow}) \\
 & + \sum_{b,t} (C_b^{Re,\uparrow} R_{b,t}^{\uparrow} + C_b^{Re,\downarrow} R_{b,t}^{\downarrow}) \\
 & + \sum_{w,t} (C_w^{Re,\uparrow} R_{w,t}^{\uparrow} + C_w^{Re,\downarrow} R_{w,t}^{\downarrow}) + \sum_{D,t} \gamma_{D,t} \quad (1)
 \end{aligned}$$

where  $p_{g,t}^s$  and  $dsr_{b,t}^s$  are the power generation of the CG  $g$  and the active power procured by the DSR program at transmission bus  $b$  within scenarios, respectively. The variables of start-up “ $st_{g,t}$ ” and shut-down “ $sd_{g,t}$ ” are calculated using the online/offline status of CGs “ $i_{g,t}$ ” as presented by Equation (2). Constraints in Equations (3) and (4) count the minimum up/down-time duration for CGs, in which  $T_{g,on}^{min}$  and  $T_{g,off}^{min}$  are the limits in hours (h). The ramp rates, including hourly upward/downward regulation limits “ $Ru_g/Rd_g$ ” and the limit of ramping from/to offline status “ $RS_g/RD_g$ ” are checked by Equations (5) and (6), respectively. The generation bounds “ $min/max$ ” of CGs are reflected by Equation (7). Constraints in Equations (8) and (9) calculate the dispatch values for inside blocks of CGs that have various generation costs. The dispatch limits of wind farms based on the maximum available wind energy within scenarios are considered by Equation (10), and

Equation (11) calculates the corresponding value for wind output at the base case scenario.

$$i_{g,t} - i_{g,(t-1)} = st_{g,t} - sd_{g,t} \quad (2)$$

$$st_{g,t} \leq i_{g,\tau}, \quad \forall t \leq \tau \leq t + T_{g,on}^{\min} - 1 \quad (3)$$

$$sd_{g,t} \leq 1 - i_{g,\tau}, \quad \forall t \leq \tau \leq t + T_{g,off}^{\min} - 1 \quad (4)$$

$$\dot{p}_{g,t}^{s_0} - \dot{p}_{g,(t-1)}^{s_0} \leq RS_g st_{g,t} + Ru_g i_{g,(t-1)} \quad (5)$$

$$\dot{p}_{g,(t-1)}^{s_0} - \dot{p}_{g,t}^{s_0} \leq RD_g sd_{g,t} + Rd_g i_{g,(t-1)} \quad (6)$$

$$P_g^{\min} i_{g,t} \leq \dot{p}_{g,t}^s \leq P_g^{\max} i_{g,t} \quad (7)$$

$$\dot{p}_{g,t}^{j,s} \leq \dot{p}_g^{j,\max} i_{g,t} \quad (8)$$

$$\dot{p}_{g,t}^s = \sum_j \dot{p}_{g,t}^{j,s} i_{g,t} \quad (9)$$

$$0 \leq \dot{p}_{w,t}^s \leq P_{w,t}^{s,\max} \quad (10)$$

$$P_{w,t}^{s_0,\max} = \sum_{s^t \geq 1} \pi_{t,s^t} P_{w,t}^{s^t,\max} \quad (11)$$

The DSR program within scenarios of uncertainties and at the base case scenario, operated by the demands located at the transmission level, is reflected by Equations (12)–(15). The parameter  $\Gamma_{b,t}$  is the coefficient of the maximum allowed demands' participation. It should be noted that this paper incorporates demand-side resources and curtailable demands as the DSR program; however, other options, i.e. the demand-shift, can be considered in the same way. Constraint in Equation (13) computes the demand of the base case scenario, and Equation (15) calculates the values of the procured active power by the DSR programs.

$$\dot{p}_{b,t}^{Dem,s} \leq P_{b,t}^{Dem,s} \quad (12)$$

$$P_{b,t}^{Dem,s_0} = \sum_{s^t \geq 1} \pi_{t,s^t} P_{b,t}^{Dem,s^t} \quad (13)$$

$$P_{b,t}^{Dem,s} - \dot{p}_{b,t}^{Dem,s} \leq \Gamma_{b,t} P_{b,t}^{Dem,s} \quad (14)$$

$$dsr_{b,t}^s = P_{b,t}^{Dem,s} - \dot{p}_{b,t}^{Dem,s} \quad (15)$$

The required reserves in upward and downward directions (compared to the dispatches of base case scenario) supplied from CGs, wind farms, and DSR programs for covering the

uncertainties are determined by Equations (16)–(21).

$$R_{g,t}^{\uparrow} \geq \dot{p}_{g,t}^s - \dot{p}_{g,t}^{s_0} \quad (16)$$

$$R_{g,t}^{\downarrow} \geq \dot{p}_{g,t}^{s_0} - \dot{p}_{g,t}^s \quad (17)$$

$$R_{w,t}^{\uparrow} \geq \dot{p}_{w,t}^s - \dot{p}_{w,t}^{s_0} \quad (18)$$

$$R_{w,t}^{\downarrow} \geq \dot{p}_{w,t}^{s_0} - \dot{p}_{w,t}^s \quad (19)$$

$$R_{b,t}^{\uparrow} \geq dsr_{b,t}^s - dsr_{b,t}^{s_0} \quad (20)$$

$$R_{b,t}^{\downarrow} \geq dsr_{b,t}^{s_0} - dsr_{b,t}^s \quad (21)$$

Since the operational cost of DSOs is shifted to the optimality check sub-problem, the model sets the free variable of active power export to the distribution grids “ $\dot{p}_{D,t}^{Exp}$ ” to the maximum negative variable during the initial iterations. So, constraint in Equation (22) limits the calculated active power exchange at the T&D interface based on a range of possible values to reduce the infeasible solution based on the thermal limit of electrical tie-lines. The sets  $To(l)$  and  $From(l)$  are the forwarding and receiving buses of lines  $l$ , while  $S_{base}$  and  $X_l$  are the base power of the per-unit system and lines' reactance (p.u.). The active power flow of transmission lines “ $\dot{p}_{l,t}^{s}$ ” is calculated by Equation (23) using the DC description, and the limits are reflected by Equation (24). Equation (25) describes the constraint on the voltage angle “ $\delta_b^{t,s}$  (rad)” of the reference bus. Also, Equation (26) considers the active power balance of buses located at the transmission grid for all scenarios, including of the base case scenario ( $s_0$ ), in which  $K$ ,  $\varphi$ , and  $T$  are the sets of generators, wind farms, and lines connected to the transmission bus  $b$ . The set  $\nu$  contains border buses exporting power to distribution grids.

$$P_{D,t}^{Exp,\min} \leq \dot{p}_{D,t}^{Exp} \leq P_{D,t}^{Exp,\max} \quad (22)$$

$$\dot{p}_{l,t}^s = S_{base} \left( \delta_{To(l)}^{t,s} - \delta_{From(l)}^{t,s} \right) / X_l \quad (23)$$

$$-P_l^{\max} \leq \dot{p}_{l,t}^s \leq P_l^{\max} \quad (24)$$

$$\delta_{Ref}^{t,s} = 0 \quad (25)$$

$$\sum_{g \in K} \dot{p}_{g,t}^s + \sum_{w \in \varphi} \dot{p}_{w,t}^s - \sum_{l \in T} \dot{p}_{l,t}^s - \sum_{D \in \nu} \dot{p}_{D,t}^{Exp} = \dot{p}_{b,t}^{Dem,s} \quad (26)$$

## 2.2 | Model of the DSOs (sub-problems)

As stated, solving the UC problem at the distribution level can be performed by DSOs using the value of intermediary

variables of export power to distribution grids. It should be noted the negative values for intermediary free variables of exported power to DSOs indicate reverse active power flow from distribution to the upstream network. The distribution grid constraints are invisible to the TSO, and the obtained values for active power trading between networks can lead to an infeasible solution and power curtailments. The feasibility check sub-problems remove the power curtailments. After removing infeasibilities, the optimality check sub-problem measures the impact of TSO's decision on the operational cost of distribution grids and sends feedbacks of selected values for the intermediary variables to the TSO. It should be noted the complete separation of the TSO and DSOs' markets make the proposed model capable of considering various uncertainties per DSOs (specified by a different index of  $k$ ) independent of the transmission level scenarios.

### 2.2.1 | Feasibility check sub-problem

The feasibility of the master solution is evaluated by this sub-problem and solved per DSOs. The obtained values for intermediary variables can violate constraints of distribution systems; however, the range of violations cannot be determined by an infeasible solution. This sub-problem defines positive variables for power curtailments and solves a feasible model to obtain violation ranges. In the objective function Equation (27),  $S_{D,t}$  is the sum of positive variables  $S_{m,t}^{k,\uparrow}$  and  $S_{m,t}^{k,\downarrow}$  (sum of the expected value of scenarios and the base case scenario), which reflect curtailments of load and curtailments of power generation, respectively. In Equation (28), the probability of the base case scenario " $\pi_{t,k_0}^D$ " is equal to one, and  $DB_m^D$  is the connectivity matrix of bus  $m$  to distribution system  $D$ . So, the non-zero values of  $S_{D,t}$  indicate the infeasibility of the master solution, and it is calculated per DSOs. Constraints of this sub-problem include Equations (28)–(37), and (41)–(47).

$$\min_{(s^{\uparrow}, s^{\downarrow})} \sum_t S_{D,t} \quad (27)$$

$$S_{D,t} = \sum_k \pi_{t,k}^D \sum_m DB_m^D \left( S_{m,t}^{k,\uparrow} + S_{m,t}^{k,\downarrow} \right) \quad (28)$$

Constraints of Equations (29) and (30) check the ramp rate limits of DGs at the base case scenario, while Equation (31) limits  $\dot{P}_{dg,t}^k$  as the generation of DGs. The  $Q_{dg}^{\min}$  and  $Q_{dg}^{\max}$  are the limits of  $q_{dg,t}^k$  as the reactive power generation of DGs, which is reflected by Equation (32). Constraint in Equation (33) defines the bounds for the production of wind farms  $\dot{P}_{wd,t}^k$  within scenarios (including the base case scenario  $k_0$ ), and Equation (34) calculates the available wind power at the base case scenario. The DSR program at the distribution level is checked by Equations (35) and (37). Also, Equation (36) determines the distribution expected load at the base case scenario.

$$\dot{P}_{dg,t}^{k_0} - \dot{P}_{dg,t}^{k_0} \leq R_{dg} \quad (29)$$

$$\dot{P}_{dg,t}^{k_0} - \dot{P}_{dg,t}^{k_0} \leq R_{dg} \quad (30)$$

$$0 \leq \dot{P}_{dg,t}^k \leq P_{dg}^{\max} \quad (31)$$

$$Q_{dg}^{\min} \leq q_{dg,t}^k \leq Q_{dg}^{\max} \quad (32)$$

$$0 \leq \dot{P}_{wd,t}^k \leq P_{wd,t}^{k,\max} \quad (33)$$

$$P_{wd,t}^{k_0,\max} = \sum_{D,(k^l \geq 1)} \pi_{t,k^l}^D DW_{wd,t}^D P_{wd,t}^{k^l,\max} \quad (34)$$

$$P_{m,t}^{Dem,k} \leq P_{m,t}^{Dem,k} \quad (35)$$

$$P_{m,t}^{Dem,k_0} = \sum_{D,(k^l \geq 1)} \pi_{t,k^l}^D BD_m^D P_{m,t}^{Dem,k^l} \quad (36)$$

$$P_{m,t}^{Dem,k} - \dot{P}_{m,t}^{Dem,k} \leq \Gamma_{m,t} P_{m,t}^{Dem,k} \quad (37)$$

The description of the AC power flow is reflected by Equations (38) and (39), in which the conductance " $G_m^n$ " and the susceptance " $B_m^n$ " are the real and imaginary parts of the admittance matrix ( $Y_m^n = G_m^n + jB_m^n$ ). The variables of  $pl_{m,n}^{t,k}$  and  $ql_{m,n}^{t,k}$  are the active and reactive power flow of distribution lines connecting buses  $m$  and  $n$  (member of set  $Z$ ). Also, the limits of the voltage magnitude " $V_{m,t}^k$ " are considered by Equation (40).

$$pl_{m,n}^{t,k} = S_{base} \left( G_m^n (V_{m,t}^k)^2 - G_m^n V_{m,t}^k V_{n,t}^k \cos(\delta_m^{t,k} - \delta_n^{t,k}) - B_m^n V_{m,t}^k V_{n,t}^k \sin(\delta_m^{t,k} - \delta_n^{t,k}) \right), \quad \forall m, n \in Z \quad (38)$$

$$ql_{m,n}^{t,k} = S_{base} \left( -B_m^n (V_{m,t}^k)^2 + B_m^n V_{m,t}^k V_{n,t}^k \cos(\delta_m^{t,k} - \delta_n^{t,k}) - G_m^n V_{m,t}^k V_{n,t}^k \sin(\delta_m^{t,k} - \delta_n^{t,k}) \right), \quad \forall m, n \in Z \quad (39)$$

$$V_m^{\min} \leq V_{m,t}^k \leq V_m^{\max} \quad (40)$$

The non-linear constraints of Equations (38) and (39) are non-convex and make the model complex. In this regard, a transformation into SOCP formulation is applied by defining auxiliary variables  $u_{m,t}^k = (V_{m,t}^k)^2/2$ ,  $H_{m,n}^{t,k} = V_{m,t}^k V_{n,t}^k \cos(\delta_m^{t,k} - \delta_n^{t,k})$ , and  $I_{m,n}^{t,k} = V_{m,t}^k V_{n,t}^k \sin(\delta_m^{t,k} - \delta_n^{t,k})$  [37]. So, the constraints Equations (38)–(40) become:

$$pl_{m,n}^{t,k} = S_{base} \left( \sqrt{2} G_m^n u_{m,t}^k - G_m^n H_{m,n}^{t,k} - B_m^n I_{m,n}^{t,k} \right), \quad \forall m, n \in Z \quad (41)$$

$$ql_{m,n}^{t,k} = S_{base} \left( -\sqrt{2} B_m^n u_{m,t}^k + B_m^n H_{m,n}^{t,k} - G_m^n I_{m,n}^{t,k} \right), \quad \forall m, n \in Z \quad (42)$$

$$\frac{(V_m^{\min})^2}{2} \leq u_{m,t}^k \leq \frac{(V_m^{\max})^2}{2} \quad (43)$$

where  $H_{m,n}^{t,k} = H_{n,m}^{t,k}$  and  $I_{m,n}^{t,k} = -I_{n,m}^{t,k}$ . Also, Equation (44) describes the relationship between  $H_{m,n}^{t,k}$  and  $I_{m,n}^{t,k}$ .

$$2\mu_{m,t}^k \mu_{n,t}^k \geq \left(H_{m,n}^{t,k}\right)^2 + \left(I_{m,n}^{t,k}\right)^2, \quad \forall m, n \in Z \quad (44)$$

The convex Equation (45) considers the thermal limit “ $S_{m,n}^{\max}$ ” for distribution lines.

$$\left(p_{m,n}^{t,k}\right)^2 + \left(q_{m,n}^{t,k}\right)^2 \leq \left(S_{m,n}^{\max}\right)^2, \quad \forall m, n \in Z \quad (45)$$

The reactive power balance is considered by Equation (46), in which  $\eta$  and  $\beta$  are the sets of DGs and T&D interface connected to distribution bus  $m$ . The balance of the active power is evaluated by Equation (47), in which  $\lambda_{m,t}^k$  is the dual variable (so-called shadow prices), and the fixed value of  $\hat{p}_{D,t}^{Exp}$  is the solution of the master problem. Also,  $\hat{p}_{m,t}^{Dem,k}$  and  $\hat{q}_{m,t}^{Dem,k}$  are the active and reactive demands located at distribution buses.

$$\sum_{dg \in \eta} q_{dg,t}^k - \sum_{n \in Z} q_{m,n}^{t,k} + \sum_{D \in \beta} q_{D,t}^{Exp} = q_{m,t}^{Dem,k} \quad (46)$$

$$\begin{aligned} & \sum_{dg \in \eta} p_{dg,t}^k + \sum_{wd \in \psi} p_{wd,t}^k - \sum_{n \in Z} p_{m,n}^{t,k} + \sum_{D \in \beta} \hat{p}_{D,t}^{Exp} + S_{m,t}^{k,\uparrow} - S_{m,t}^{k,\downarrow} \\ & = \hat{p}_{m,t}^{Dem,k}, \quad \forall m \in \chi(D) \rightarrow (\lambda_{m,t}^k) \end{aligned} \quad (47)$$

As illustrated, if the objective function of the feasibility check sub-problem is positive for each distribution system, it reveals that the solution (the obtained values for intermediary variables by the master problem) is infeasible. Consequently, a Benders infeasibility cut will be generated by Equation (48). The infeasibility cut will limit the variables of  $\hat{p}_{D,t}^{Exp}$  in the master problem based on the measured infeasibility and values of shadow prices at the corresponding buses.

$$\hat{S}_{D,t} - \sum_m DB_m^D \sum_k \hat{\lambda}_{m,t}^k \left( \hat{p}_{D,t}^{Exp} - \hat{p}_{D,t}^{Exp} \right) \leq 0 \quad (48)$$

## 2.2.2 | Optimality check sub-problem

This problem evaluates the operating cost of distribution systems based on the calculated values for power trading with the TSO. The objective function Equation (49) obtains an upper bound of the overall cost for distribution systems. Constraint Equation (50) calculates the expected value of cost per distribution system (the weighted sum of values incurred within scenarios), and it consists of the cost of energy and reserves provided by different resources. The  $GD_{dg}^D$  is the connectivity matrix of distributed generators  $dg$  to the distribution system  $D$ . Constraints of this sub-problem are Equations (29)–(37), (41)–(46),

and (50)–(58).

$$\min_{\left(\begin{smallmatrix} p,q,dsr, \\ R,u,H,I \end{smallmatrix}\right)} \sum_t F_{D,t} \quad (49)$$

S.t. Equations (29)–(37), (41)–(46), and (50)–(58)

$$\begin{aligned} F_{D,t} = & \sum_{dg, t, (k \geq 1)} \pi_{t,k}^D GD_{dg}^D C_{dg}^{En} p_{dg,t}^k \\ & + \sum_{dg,t} GD_{dg}^D \left( C_{dg}^{Re,\uparrow} R_{dg,t}^{\uparrow} + C_{dg}^{Re,\downarrow} R_{dg,t}^{\downarrow} \right) \\ & + \sum_{m,t, (k \geq 1)} \pi_{t,k}^D DB_m^D C_m^{En} dsr_{m,t}^k \\ & + \sum_{m,t} DB_m^D \left( C_m^{Re,\uparrow} R_{m,t}^{\uparrow} + C_m^{Re,\downarrow} R_{m,t}^{\downarrow} \right) \\ & + \sum_{wd,t} DW_{wd}^D \left( C_{wd}^{Re,\uparrow} R_{wd,t}^{\uparrow} + C_{wd}^{Re,\downarrow} R_{wd,t}^{\downarrow} \right) \end{aligned} \quad (50)$$

The required reserve capacities in upward and downward directions and for dispatching the various resources within all scenarios of uncertainties are determined by Equations (51)–(56).

$$R_{dg,t}^{\uparrow} \geq p_{dg,t}^k - \hat{p}_{dg,t}^{k_0} \quad (51)$$

$$R_{dg,t}^{\downarrow} \geq \hat{p}_{dg,t}^{k_0} - p_{dg,t}^k \quad (52)$$

$$R_{wd,t}^{\uparrow} \geq p_{wd,t}^k - \hat{p}_{wd,t}^{k_0} \quad (53)$$

$$R_{wd,t}^{\downarrow} \geq \hat{p}_{wd,t}^{k_0} - p_{wd,t}^k \quad (54)$$

$$R_{m,t}^{\uparrow} \geq dsr_{m,t}^k - dsr_{m,t}^{k_0} \quad (55)$$

$$R_{m,t}^{\downarrow} \geq dsr_{m,t}^{k_0} - dsr_{m,t}^k \quad (56)$$

The values of active power procured by DSR programs at distribution grids “ $dsr_{m,t}^k$ ” are calculated by Equation (57). Constraint of Equation (58) evaluates the active power balance of distribution buses, in which  $\mu_{m,t}^k$  is the dual variable. Since the feasibility check sub-problems have removed all power curtailments, the power balance constraint Equation (58) will always be feasible.

$$dsr_{m,t}^k = P_{m,t}^{Dem,k} - \hat{p}_{m,t}^{Dem,k} \quad (57)$$

$$\begin{aligned} & \sum_{dg \in \eta} p_{dg,t}^k + \sum_{wd \in \psi} p_{wd,t}^k - \sum_{n \in Z} p_{m,n}^{t,k} + \sum_{D \in \beta} \hat{p}_{D,t}^{Exp} \\ & = \hat{p}_{m,t}^{Dem,k}, \quad \forall m \in \chi(D) \rightarrow (\mu_{m,t}^k) \end{aligned} \quad (58)$$



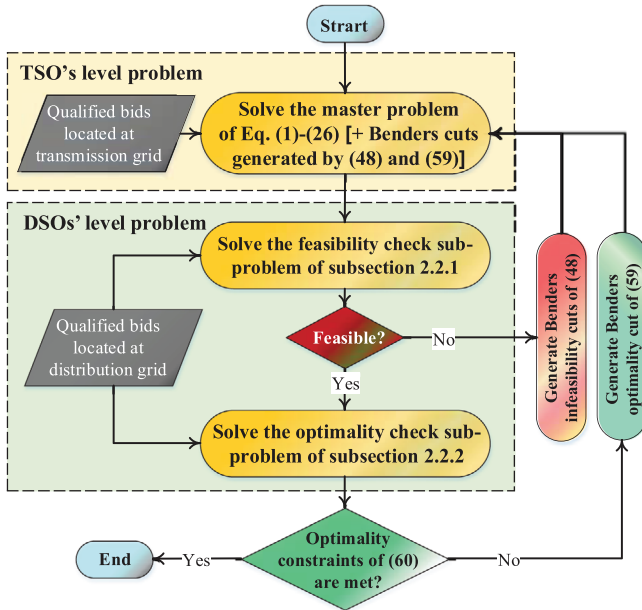


**FIGURE 1** Flowchart of the solving process in the privacy-preserving platform of TSO-DSO coordinated scheduling for energy and reserve

The optimality cuts will be generated using Equation (59) until the convergence criterion Equation (60) is met, and the gap between the upper bound and lower bound values for DSOs' cost reduce lower than a predefined threshold. In fact, optimality cuts are the feedback of the obtained values for intermediary variables and set constraints (using obtained values of DSOs' cost and shadow prices at the T&D interface) on calculating the lower bound of  $\gamma_{D,t}$  by the master problem in the next iteration. Further explanation of the mathematical basis on shaping Benders cuts can be found in [38, 39].

$$\gamma_{D,t} \geq \hat{F}_{D,t} - \sum_{m,(k \geq 1)} DB_m^D \hat{\mu}_{m,t}^k \left( p_{D,t}^{Exp} - \hat{p}_{D,t}^{Exp} \right) \quad (59)$$

$$2 \left( \hat{F}_{D,t} - \hat{\gamma}_{D,t} \right) / \left( \hat{F}_{D,t} + \hat{\gamma}_{D,t} \right) \leq \varepsilon \quad (60)$$

### 2.3 | The proposed privacy-preserving platform

The master problem will be solved by the TSO, or independent market operator (IMO) based on regulatory rules, while DSOs can solve the sub-problems. The flowchart of Figure 1 presents the solving algorithm of the proposed model. The algorithm is initiated by solving the master problem. After that, feasibility check sub-problems evaluate the master solution to be feasible for distribution grid constraints. The infeasibility cuts are added to the master problem to remove power curtailments, and the iterative process is continued to eliminate all curtailments. After that, the algorithm solves the optimality check sub-problem and shapes the optimality cuts. The master problem is solved again considering the added cuts, and these steps are repeated until the convergence criterion is met. After solving the model, the

cost of energy trading is calculated using the intermediary variables of power exchange at the T&D interface and the corresponding LMPs. Here, the LMPs are the dual variables (shadow prices) of the power balance constraints Equations (26) at the transmission level.

## 3 | NUMERICAL RESULTS

This section evaluates the proposed hybrid centrally-supported decentralized scheme for TSO-DSO coordination on a modified IEEE 24-bus test system. Five distribution systems are installed at buses 6, 13, 15, 18, and 19. Figure 2 presents a single-line diagram of the proposed test system, and data of the proposed test system is prepared in [40]. Also, the scenarios of load curves and available wind energy are presented in the Appendix. The proposed model and all experiments are performed using General Algebraic Modelling System (GAMS) on a laptop with Intel i7-core 2.4 GHz and 8 GB of RAM. The master mixed-integer linear programming problem (MILP), the SOCP of the feasibility check sub-problem, and the SOCP model of optimality check sub-problem are solved using the CPLEX, GUROBI, and MOSEK solvers of the GAMS, respectively. Although all of these solvers can solve both the MILP and SOCP models, they have different accuracy, speed, and options. Based on our experiment, the used combination of solvers result in the best performance in accuracy and solution time for the master problem and sub-problems. The duality gaps of the master and sub-problems are selected equal to zero.

### 3.1 | Scenario generation

This section will describe the scenario generation method used for addressing the fluctuation of wind output and the load forecasting errors. The proposed sampling method is started with generating a large number of random numbers. In this paper, the samples of wind power fluctuation and load forecasting errors are generated using Weibull and normal distribution functions, respectively. Also, the standard deviation of sampling increases uniformly (between 0 and 0.1) to reflect the increase in prediction error based on the remaining time interval to the scenario realizations. The prediction of uncertain parameters is beyond the scope of this paper; hence, the mean value of samples for wind is selected based on meteorological prediction, and original load curves of grids are assumed as the mean value for sampling hourly demand. Since the consideration of too many scenarios complicates the stochastic model, a scenario reduction based on probability distance, which is described in [2, 3], is applied to select the most effective scenarios. The index of probability distance is defined as the absolute difference to all other scenarios multiplied by its probability. The scenario with the minimum value for the index of probability distance will be omitted, and its probability is added to the corresponding scenarios with the maximum similarity. In this paper, 1000 samples are generated for each wind farm and hourly load, and each scenario has an equal probability of 0.001. After that, the

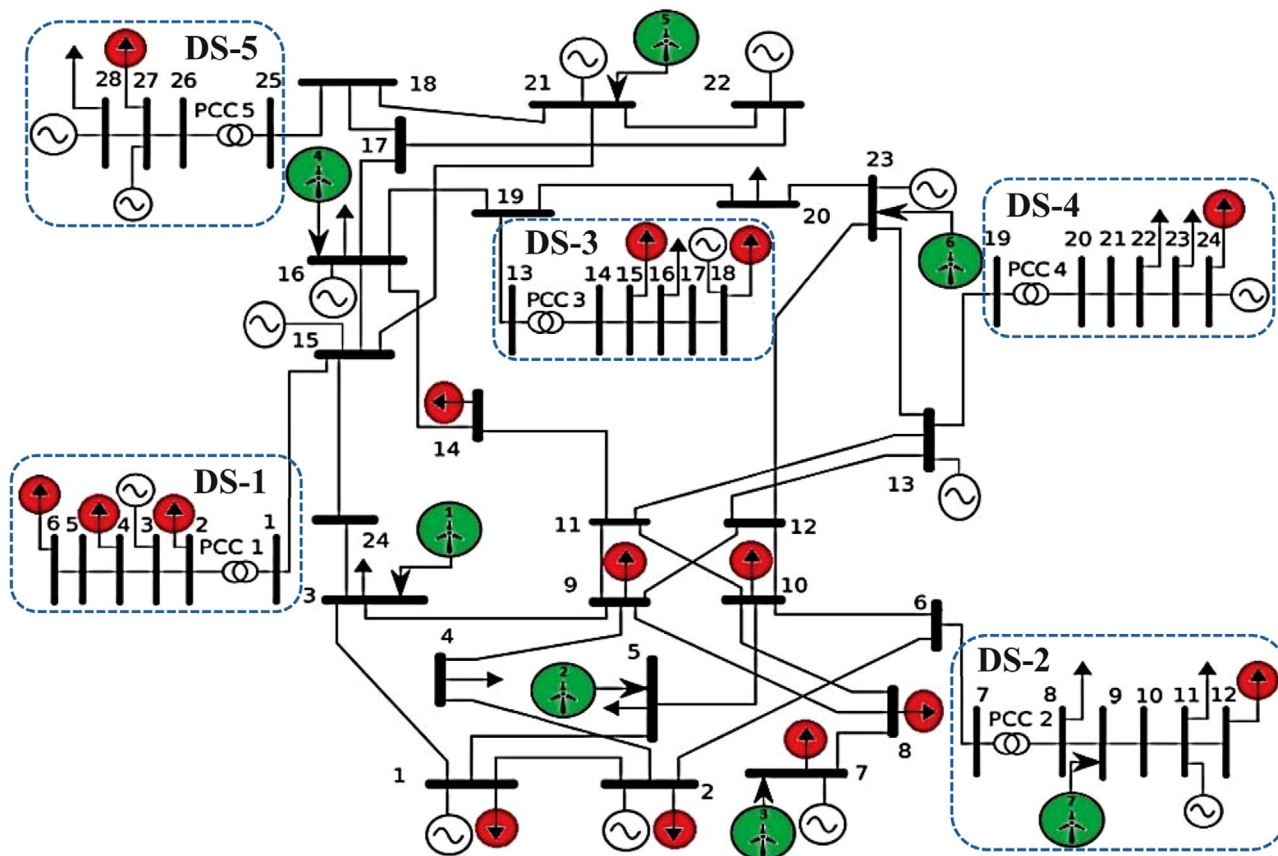


FIGURE 2 Single-line diagram of the modified IEEE 24-bus test system with five downstream distribution systems

number of scenarios is reduced by combining samples with the maximum similarities. For simplicity, we assume the samples of various stochastic parameters related to the same energy system are arranged in a string, and then the scenario reduction is performed.

### 3.2 | Results

Different aspects of the results, including operational costs, TSO-DSO interactions, costs of agents, generation mix of the units, and other outputs of the UC problem, are analyzed in the remaining of this section. Here we consider two following cases for evaluating the proposed model: (a) Case-1: a deterministic formulation with no uncertainties (b) Case-2: a stochastic model considering uncertainties of load and wind.

#### 3.2.1 | Case-1

Since previous models do not consider uncertainties and reserves, a deterministic implementation (scheduling for the base case scenario with the expected values of the stochastic parameters) is used to evaluate the advantages of the proposed platform compared to other implementations. The proposed

four strategies include fully centralized, centralized with prior dispatching of DSOs, decentralized, and the proposed hybrid model of this paper. Strategy-A considers the integrated centralized scheduling of TSO and DSOs without any priority of SOs in using resources. Strategy-B presents the centralized model with a hierarchical organization, in which DSOs first manage their grid using local resources. Then, joint T&D scheduling is run with the remaining capacity of DERs. Strategy-C is implemented based on the decentralized model of [17]; however, this can be extended to all platforms that use the merit-order list of qualified bids based on prices. In that model, boundaries for the power flow at the T&D interface are obtained considering constraints of distribution grids (based on ranges of DERs' generations). After that, the calculated bounds of DERs and all demands are assumed to be available at the transmission bus, and central dispatching is performed using the qualified bids without considering DSOs' grid constraints. Strategy-D is the proposed hybrid model presented by this paper, and it uses the decomposition-based framework to address restrictions of the model complexity and data-sharing. The description of the defined strategies is itemized in Table 2.

Table 3 presents and compares the operational costs evaluated by different strategies. Strategy-A operates the integrated model of T&D systems and calculates the best optimal solution for overall system scheduling. Since Strategy-B considers a

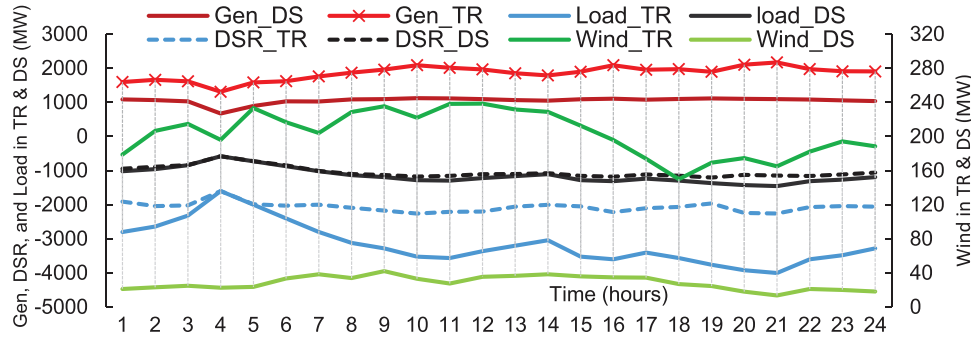


**FIGURE 3** Dispatches of suppliers in transmission and distribution systems for Strategy-D

**TABLE 2** Model specifications of different strategies

	Strategy-A	Strategy-B	Strategy-C [17]	Strategy-D*
Type	Centralized	Centralized	Decentralized	Hybrid
Prior-dispatch	No	By DSOs	No	No
DS-grid	Integrated	Integrated	Pre-qualified	Decomposed
Complexity	High	High	Low	Medium
Privacy issue	Yes	Yes	No	No

\*Proposed platform proposed by this paper.

priority for DSOs in the utilization of local resources, the grid local management does not lead to the best optimal solution for the system. The reason is that considering the power exchange with the upstream network alleviates the tied constraints of radial AC power flow. For Strategy-C, the validation of the calculated values of DERs' dispatches is performed based on distribution grid constraints. As it can be seen, the calculated values for DERs are not meet the distribution constraints; so, an optimal re-dispatch is applied based on contracted power flow at the T&D interface. Hence, the calculated, realized, and deviations of operational cost per SOs are reported for this strategy. In this regard, DSOs are obligated to clear the contracted value, where the higher charges for regulation services can further increase the operational costs. As it can be seen, considerable deviations are obtained compared to the calculated operational costs of four DSOs, and a 5.6% deviation in the overall cost is obtained by applying this strategy. This issue does not happen in other structures, where the calculated and realized values are the same. As it can be seen, the operational costs obtained by the decomposed model of Strategy-D for the overall system and DSOs are very close to the values of Strategy-A as the most optimal solution. In addition, it is revealed the proposed coordinated platform reduces the operational costs for all SOs (up to 19.4% for DS-5) compared to the isolated operating case of T&D networks, while a 3.3% reduction is achieved for the system overall cost.

Table 4 compares the obtained values for the total import and export active energy at the T&D interface for different strategies. Based on the features of the applied schemes, Strategy-C is expected to set the power flow of the T&D interface to the maximum values; because the values in this strategy are obtained

only based on prequalification with minimum restrictions. In all cases, DS-1 and DS-5 export considerable amounts of energy, while the TSO imports the sum of exported power of distribution systems.

### 3.2.2 | Case-2

The stochastic implementation of the proposed model for privacy-preserving scheduling of T&D grids is evaluated in this section. The trend of dispatches of various sources is presented for Strategy-D in Figure 3. This figure maps the scale of using various technologies in supplying demands. The adjusted demand values after the DSR program compared to the load profile are presented with negative signs. As it can be seen, the DSR participation in both levels reduces variations of the load profile. The main power supplier at the transmission and distribution systems are CGs and DGs, respectively. Also, wind farms participate in energy supply in both T&D networks.

The total values of energy generation and trading of SOs are presented in Table 5 for Strategy-D. As it can be seen, DS-1 and DS-5 export active energy, while DS-2, DS-3, and DS-4 import energy from the upstream grid. The net of active energy exchanges with distribution grids obtains a 275 MWh of energy import for the TSO. The maximum value of energy exchange between systems is 3712 MWh calculated for DS-5. The total reactive energy import of distribution grids is positive for all DSOs, and the total reactive energy supply is 2205 MVarh for the TSO. The presented values of active and reactive energy loss show acceptable ranges, and the maximum values of active energy loss are calculated for DS-1 and DS-5 with 159 MWh (1.95%) and 196 MWh (1.58%), respectively. Also, the total active and reactive energy of CGs, DGs, and wind farms are reported in Table 5. The highest values of DSR programs have been calculated for DS-1 with 1160 MWh and DS-3 with 591 MWh. Besides, the value of the DSR program at the transmission level is 26,184 MWh.

Figure 4 compares the energy prices at the T&D interfaces with the average energy price of the transmission grid. As it can be seen, for DS-1 and DS-5, the electricity prices at the T&D interface are lower than the average price of the transmission grid. The active power generation of distribution grids DS-1 and DS-5 is exported to use by the TSO. The electricity prices

**TABLE 3** Comparison of the total values of cost obtained by different strategies

	Isolated operation	Strategy-A	Strategy-B	Strategy-C			Strategy-D	
		Realized (\$)	Realized (\$)	Calculated (\$)	Realized (\$)	Dev. (%)	Realized (\$)	CIO* (%)
DS-1	122,434	107,697	93,287	144,146	129,058	11.7	107,698	13.7
DS-2	149,388	138,780	149,388	15,071	181,652	91.7	138,782	7.6
DS-3	128,952	125,592	128,952	209,739	141,814	47.9	125,593	2.7
DS-4	171,058	147,929	171,058	48,511	179,738	73.0	147,936	15.6
DS-5	105,615	88,485	60,519	182,709	119,709	52.6	88,487	19.4
TR	1,961,084	1,945,004	1,989,835	1,954,663	1,954,663	0.0	1,945,004	0.8
Overall cost	2,638,531	2,553,487	2,593,039	2,554,839	2,706,634	5.6	2,553,498	3.3

\*CIO = Compared to the isolated operating case.

**TABLE 4** Comparison of active energy import (Imp.) and export (Exp.) of system operators in MWh calculated by different strategies

	Strategy-A		Strategy-B		Strategy-C		Strategy-D	
	Imp.	Exp.	Imp.	Exp.	Imp.	Exp.	Imp.	Exp.
DS-1	0	2452	0	1941	561	3270	0	2446
DS-2	1887	0	0	0	92	2619	1887	0
DS-3	1335	0	0	0	268	1869	1334	0
DS-4	2274	0	0	0	0	500	2269	0
DS-5	0	3892	0	3708	1121	1863	0	3895
TR	6344	5496	5649	0	10,121	2042	6341	5490

**TABLE 5** Total energy in different SOs for Strategy-D—the units of active energy (P) in MWh and reactive energy (Q) in MVarh

	System operators					
	DS-1	DS-2	DS-3	DS-4	DS-5	TR
Exp.* (P)	-2318	2040	1448	2267	-3712	-275
Exp. (Q)	330	438	576	356	506	-2205
Loss (P)	159	74	32	85	196	—
Loss (%P)	1.95	1.49	0.79	1.83	1.58	—
Loss (Q)	39	28	11	21	54	—
Gen (P)	7005	2064	1994	2115	12,091	44,508
Gen (Q)	1375	1267	1129	1348	631	—
Wind	0	679	0	0	0	4873
DSR	1160	167	591	266	284	26,184
Load (P)	5688	4875	4000	4563	8468	75,877

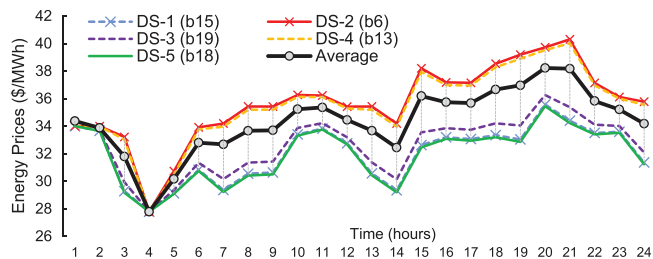


**FIGURE 4** The average value of energy prices of the transmission and distribution systems in Strategy-D

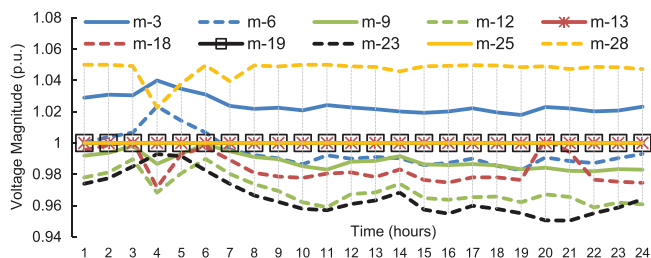


**FIGURE 5** The voltage profile related to different buses of distribution systems in per-unit (p.u.) for Strategy-C

at the T&D interface of distribution systems DS-2 and DS-4 are higher than the average transmission electricity price, and DSOs import active power from the upstream network. Also, the energy price of the DS-3 interface is lower than the average value of the upstream network; however, energy enters from the transmission system to the distribution system. The reason is that DS-3 is near two wind farms at the transmission system, and the model optimizes the scheduling of the whole energy system without any priority of SOs; consequently, low price energy is imported to be used the DSO.

The voltage profiles of distribution networks are presented in Figure 5 during 24 h of the operation horizon. The distribution reference buses 1, 7, 13, 19, and 25 are points of connection to the upstream network, and the value of one per-unit is assumed for their voltage magnitudes. So, due to the consideration of DC power flow at the transmission level, coordination of voltage magnitude and angles between different SOs is not reflected in this paper. However, capacitor banks, installed at the transmission level, and tap-changing transformers can be employed to regulate the voltage of boundary nodes; hence, the complementary actions will be coordinated through balancing and real-time markets. As it can be seen, the voltage profiles of all distribution systems are maintained within the feasible range of 0.95–1.05 (p.u.) during the whole operation period. Also, distribution bus 3 in DS-1 and bus 28 in DS-5 have the highest voltage magnitude because of the significant power generation dispatches at the locations.

Figure 6a,b shows the hourly active and reactive power exchange between distribution systems and the transmission grid, while the positive and negative values present DSO's

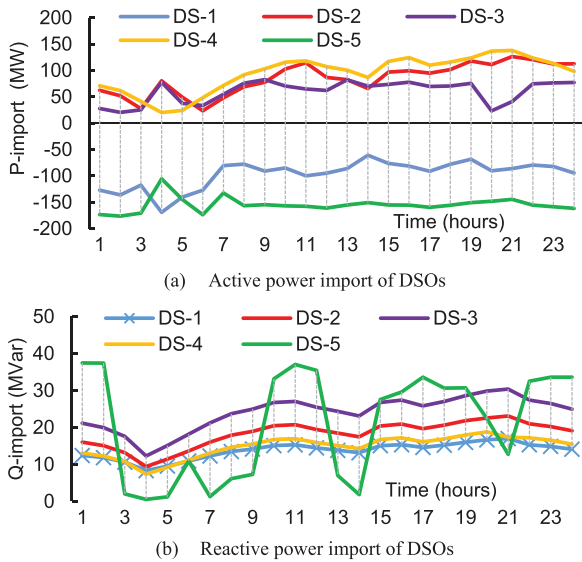


**FIGURE 6** Hourly DSOs' import of active and reactive power from TSO's grid in Strategy-D (negative values indicate the reverse flow as the export)

**TABLE 6** Costs of supplying energy and reserves per SOs and different resources in Strategy-D

	Energy (\$)			Reserve (\$)			
	Gen	DSR	Trade	Gen	Wind	DSR	Total
DS-1	150,434	33,724	-73,851	1732	0	3247	115,286
DS-2	66,008	3050	73,965	3414	1853	1598	149,888
DS-3	61,519	20,494	47,131	4476	0	0	133,620
DS-4	64,191	3929	82,395	639	0	1271	152,425
DS-5	206,321	1851	-118,776	4320	0	1467	95,183
TR	1,156,323	822,428	-10,864	18,975	8628	80,588	2,076,078
Total	1,704,796	885,476	0	33,556	10,481	88,171	2,722,480

import and export from the transmission level power system in both figures. The results show that DS-2, DS-3, and DS-4 import, while DS-1 and DS-5 export active power to the upstream network during the operation period. The maximum values in import and export active power belong to DS-4 and DS-5, respectively. The DSR program and the large installed capacity of DGs play vital roles in distribution grids DS-1 and DS-5 for supplying active power to the transmission network, respectively. Figure 6b shows that the reactive power flow direction is from the transmission grid to distribution systems, and the maximum reactive power import is 37 MVar and calculated for DS-5.

The breakdown of operating costs, including the values for energy and reserve, is shown in Table 6 for different SOs and various suppliers. The cost of active power trading between SOs is calculated using LMPs at the T&D interfaces and the values of power exchange. Also, the net energy trading costs of DSOs obtain the TSO's share equals  $-\$10,864$ . Although we have seen that the net of TSO energy exchange with distribu-

**TABLE 7** Comparison of the operational costs per SOs calculated for the Strategy-D with Strategy-A

	Centralized (Strategy-A)			Hybrid (Strategy-D)		
	Op.* cost	Trade	Total	Op.* cost	Trade	Total
DS-1	189,443	-74,671	113,230	189,137	-73,851	115,286
DS-2	73,550	75,545	147,737	75,923	73,965	149,888
DS-3	83,361	50,267	132,205	86,488	47,131	133,619
DS-4	69,677	82,709	152,563	70,031	82,395	152,426
DS-5	218,919	-124,226	94,654	213,959	-118,776	95,183
TR	2,087,309	-9,624	2,081,869	2,086,942	-10,863	2,076,079
Overall	2,722,258	0	2,722,258	2,722,480	0	2,722,480

\*Operational cost.

tion grids was 275 MWh (based on Table 5), the obtained net value of the energy trading cost for the TSO is negative. The reason is that LMPs are changing during the operation period, and the model optimizes the overall T&D systems rather than optimizing individual SOs.

The highest DSOs' operational cost is \$152,426 obtained for DS-4, and the minimum value is \$95,183 calculated for DS-5 (with the highest value of negative energy trading cost). The breakdown of reserve cost shows that the highest value of reserve costs are obtained for DSRs in DS-1, DS-4, and the TSO, and the highest values dedicate to DGs in DS-2, DS-3, and DS-5. Besides, the highest value of reserve cost is \$6,865 obtained for DS-2. The TSO's operational cost is \$2,076,078, and the system's overall cost is \$2,722,480, calculated for supporting energy and reserves for the whole energy system.

Table 7 compares the costs obtained by the hybrid model of Strategy-D developed by this paper to the centralized model of Strategy-A as the most optimal solution to evaluate the performance of the proposed stochastic implementation. As it can be seen, the obtained values by hybrid model for the operational cost, trading costs, total costs per SOs, and the overall cost of the system are very close to the centralized implementation of Strategy-A. The difference in the overall operational cost of T&D systems is about \$222, which is ignorable in comparison to the most optimal value of \$2,722,258 calculated for Strategy-A. So, this evaluation reveals that the proposed stochastic model can also obtain the results economically very close to the most optimal solution.

The values of deployed reserves in the transmission and five distribution systems are presented in Figures 7 and 8, respectively. At the transmission level, both CGs and DSRs supply a large share of reserves in the upward direction, and the downward reserve capacities are mostly provided by DSRs. The participation of the wind farm in the distribution system DS-2 is more highlighted in supplying upward reserves. As it can be seen, based on the selected strategy of shared balancing responsibility, the operators of T&D systems provide the required reserve capacities from their network resources. However, setting the base operation point for the energy exchange between networks and the expected cost of energy supply in various

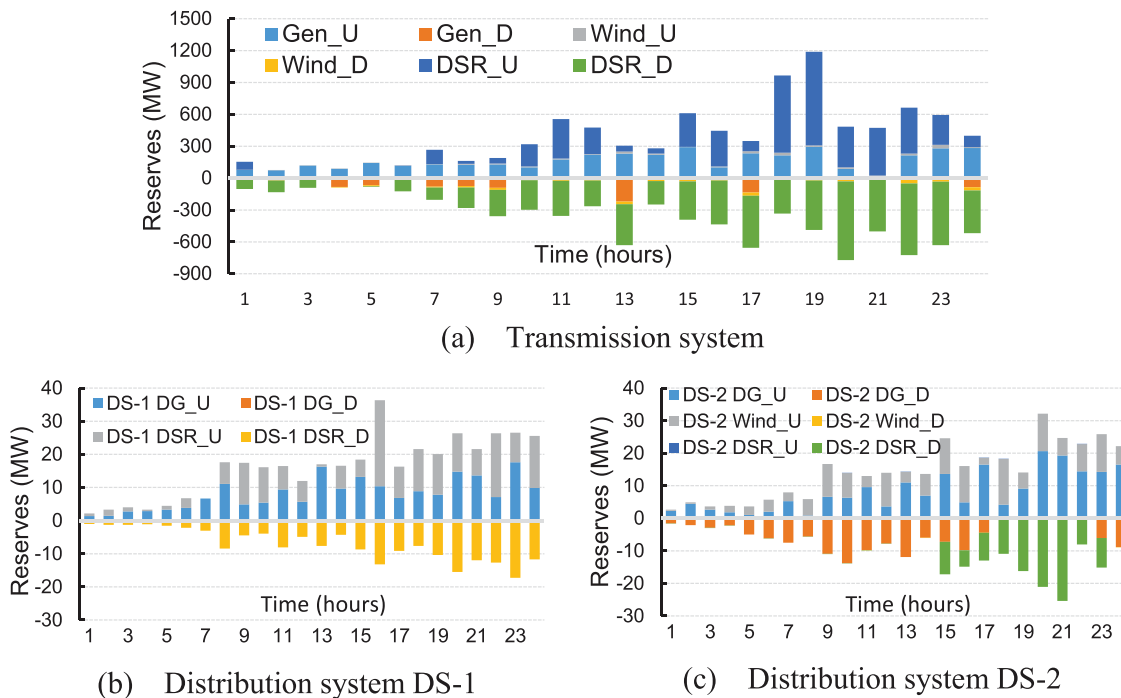


FIGURE 7 Reserves at the transmission system and distribution systems DS-1 and DS-2 (U: upward direction/D: downward direction)

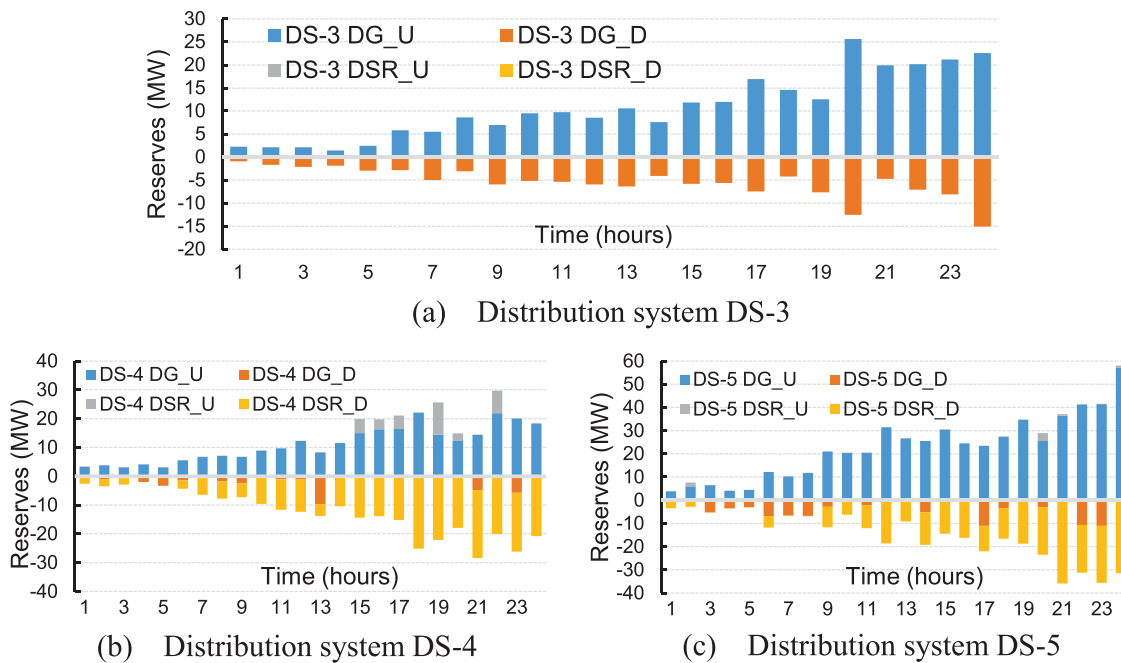


FIGURE 8 Reserves at distribution systems DS-3, DS-4, and DS-5 (U: upward direction/D: downward direction)

scenarios of uncertainty can perform a preventive role to reach an optimal solution regarding the deployed reserves in T&D networks.

The power supply within scenarios is described in Tables 8 and 9 for the transmission and distribution systems, respectively. It can be seen, the values of active power generations meet the corresponding demand plus the power loss (for DSOs’

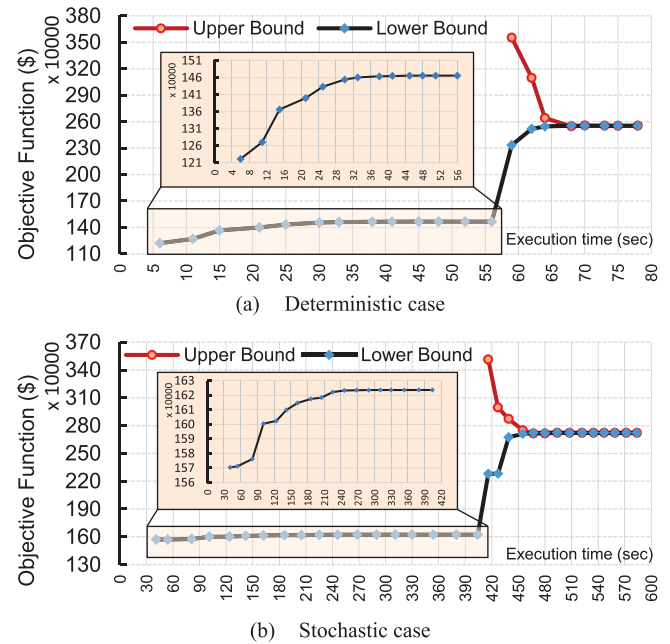
grids) in each scenario in both transmission and distribution systems. Also, the changes to the base dispatch are lower than the deployed reserves for each resource, which shows the corresponding values are sufficient for covering all scenarios in both upward and downward directions. In Table 8, it can be seen that the base dispatches are calculated close to the first scenario, which is predicted to have a high probability of

**TABLE 8** Active power dispatches in the transmission system within scenarios at hour 20

	Scenarios				Reserve	
	$s_0$	$s_1$	$s_2$	$s_3$	U	D
Probability	—	0.485	0.225	0.29	—	—
Generators	2102	2189	2189	2102	87	0
Wind farms	175	188	157	158	13	18
DSR	1682	2066	1547	941	384	741
Exp. to DSOs	33	33	33	33	—	—
Load	3925	4410	3860	3168	—	—

**TABLE 9** Active power dispatches of distribution systems within scenarios at hour 20

		Scenarios					Reserve		
		$k_0$	$k_1$	$k_2$	$k_3$	$k_4$	$k_5$	U	D
DS-1	Probability	—	0.235	0.13	0.16	0.31	0.165	—	—
	DG DS-1	285	285	290	300	300	300	15	0
	DSR DS-1	106	90	90	90	93	116	10	16
	Loss	6.5	5.9	6.1	6.5	6.2	5.9	—	—
	Exp. to TSO	90	90	90	90	90	90	—	—
	Load	294	279	284	293	297	320	—	—
DS-2	Probability	—	0.29	0.2	0.315	0.085	0.11	—	—
	DG DS-2	79	91	79	100	100	79	21	0
	Wind DS-2	18	26	24	29	20	18	11	0
	DSR DS-2	46	25	25	27	46	25	0	21
	Loss	2.5	2.4	2.5	2.4	2.1	3.2	—	—
	Exp. to TSO	-111	-111	-111	-111	-111	-111	—	—
DS-3	Load	252	251	237	265	275	230	—	—
	Probability	—	0.16	0.205	0.09	0.285	0.26	—	—
	DG DS-3	74	61	76	100	74	78	26	13
	DSR DS-3	111	111	111	111	111	111	0	0
	Loss	0.9	0.9	0.9	1.1	6.9	1.0	—	—
	Exp. to TSO	-24	-24	-24	-24	-24	-24	—	—
DS-4	Load	207	195	210	233	201	211	—	—
	Probability	—	0.14	0.235	0.145	0.16	0.32	—	—
	DG DS-4	88	93	100	88	100	100	12	0
	DSR DS-4	18	0	7	0	0	20	2	18
	Loss	6.3	6.3	6.3	6.2	6.2	6.4	—	—
	Exp. to TSO	-137	-137	-137	-137	-137	-137	—	—
DS-5	Load	236	224	238	219	231	251	—	—
	Probability	—	0.145	0.155	0.185	0.175	0.34	—	—
	DG DS-5	574	574	571	591	600	591	26	3
	DSR DS-5	21	0	0	0	3	24	3	21
	Loss	8.7	9.5	9.6	9.9	9.3	9	—	—
	Exp. to TSO	148	148	148	148	148	148	—	—
Load	438	417	413	433	445	458	—	—	

**FIGURE 9** Convergence of the proposed model in (a) deterministic case (b) stochastic case

occurrence. As Table 9 illustrates, this is not necessarily happening in all scenarios, and the corresponding expected costs and other constraints play vital roles in setting the base value of the energy and reserves in both transmission and distribution systems.

Figure 9 presents the convergence trend of the proposed model in the term of algorithm execution time and for both the deterministic and stochastic cases. The value of the lower upper bounds corresponds to the objective function of the master problem, and the upper bound is calculated using the costs obtained by the optimality check sub-problems (available only after removing all infeasible solutions). As it can be seen, the execution time for the deterministic case was 78 seconds in 21 iterations, while the stochastic model converged in 584 s and 32 iterations. It should be noted, the initial iterations of the solving process are dedicated to achieving a feasible solution that can be improved by using acceleration techniques presented in [2, 3]. Since the solution time is more critical in balancing and near real-time market the incorporation of acceleration techniques and comparison of solution time with other decentralized platforms will be investigated in future studies.

## 4 | CONCLUSION

This paper investigated a stochastic platform for coordinated scheduling of energy and reserve for the TSO and DSOs. A hybrid centrally-supported decentralized approach is applied to relieve the complexity of the model and address the privacy issue of the system operators. Since active and reactive power

flows are highly interdependent, the AC power flow of distribution grids is calculated using the SOCP relaxation method. The implementation of the proposed model on the test system leads to the following conclusions:

- The application of a decomposed framework reduces the complexity of the stochastic scheduling for integrated T&D systems, in which DSOs can solve the distribution level sub-problems. The separated platform makes it possible to consider various scenarios of uncertainties in each power system independently;
- The evaluation of results obtained by former strategies reveals that the centralized type with the hierarchical priority of DSOs for dispatching local resources can lead to higher operational costs. Also, the validation of results obtained by decentralized type (which considers DSOs' network constraints only in the prequalification process) shows a potential risk of large deviations in costs (up to 91.7% for DSOs and 5.6% in the overall cost) and state variables. The proposed platform of this paper solves these issues, and the solution is feasible regarding both T&D grid constraints. Also, the optimality of results obtained by the decomposed platform is compared and justified to the original centralized model;
- The coordinated model of scheduling TSO and DSOs improves the operating costs up to 19.4% for DSOs and 3.3% for the overall cost of the system compared to the separated operation of networks;
- The sufficiency of the deployed reserves is validated per scenarios for T&D systems, where the system operators are responsible for balancing their grids based on the selected TSO-DSO coordination scheme in this paper;
- The operational cost per distribution system is calculated using LMPs at the T&D interface. Also, bidirectional energy trading between SOs is achieved by the proposed model, where two distribution systems export and three import power from the transmission grid. The TSO imports energy based on the net value of trading with DSOs;
- The market liquidity is increased by the proposed platform, which none of the SOs have any priorities in using resources either in transmission or distribution grids. Also, the result shows that the model optimizes the overall cost of T&D systems rather than minimizing charges for individual market parties;
- The voltage profiles are calculated within limits, and the active power loss is below 2% in all distribution grids.

The future direction of this study includes the extension of the proposed model for trading flexibility services between energy systems based on regulatory frameworks of different flexibility markets. Also, our future researches will study the implementation of the proposed model on different test systems and the coordination of various SOs' voltages.

## NOMENCLATURE

### Indices and sets

$g, dg, j$	Indices of generators and DGs, and generators inside blocks
$w, wd$	Indices of wind farms in transmission and distribution grids
$m, D$	Indices of distribution buses and distribution systems
$b, Ref, l$	Indices of transmission buses, reference bus, and lines
$En/Re$	Indices of labels for energy and reserve
min/max	Indices of minimum and maximum limits of variables
$\uparrow / \downarrow$	Indices of regulation in upward/downward directions
$off, on$	Indices of offline and online statuses of units
$(t/\tau), base$	Indices of time and the base power of per-unit system
$(s/s'), \kappa$	Indices of scenarios at T&D levels ( $s_0/\kappa_0$ = base case scenario)
$TR, DS$	Indices of labels for T&D systems
$Exp$	Index of export from transmission system
$Dem$	Index of demand
$To/From$	Sets of forwarding and receiving buses of line $l$
$K, \varphi, T$	Sets of generators, wind farms, and lines connected to bus $b$
$v, \beta$	Sets of transmission buses exporting and distribution buses importing power at T&D interface
$Z$	Sets of buses connected through distribution lines
$\chi$	Sets of buses connected to distribution system $D$
$\eta, \psi$	Sets of DGs and wind farms connected to distribution bus $m$
Variables	
$p_{l,t}^s, p_{m,n}^{t,k}$	Active flow of transmission/distribution lines (MW)
$i_{g,t}, s_{g,t}^t, s_{d,g,t}$	Generators' status for on/off status and start-up/shut-down
$p_{g,t}^s, p_{dg,t}^k$	Active power of generators and DGs (MW)
$R_{g,t}^{(\uparrow/\downarrow)}, R_{dg,t}^{(\uparrow/\downarrow)}$	Reserve capacities of generators and DGs (MW)
$q_{m,n}^{t,k}, q_{dg,t}^k$	Reactive flow of lines and generation of DGs (MVar)
$p_{w,t}^s, p_{wd,t}^k$	Active power generation of wind farms (MW)
$R_{w,t}^{(\uparrow/\downarrow)}, R_{wd,t}^{(\uparrow/\downarrow)}$	Reserve capacities provided by wind farms (MW)
$p_{D,t}^{Exp}, q_{D,t}^{Exp}$	Active (MW) /reactive (MVar) power at T&D interface
$\delta_b^{t,s}, \delta_m^{t,k}$	Angle of buses at T&D grids (rad)
$dsr_{b,t}^s, dsr_{m,t}^k$	Active power procured by DSR program (MW)
$V_{m,t}^k, u_{m,t}^k$	Voltage magnitude of buses and auxiliary variable for square of voltage magnitude of buses (p.u.)
$R_{b,t}^{(\uparrow/\downarrow)}, R_{m,t}^{(\uparrow/\downarrow)}$	Reserve capacities of DSR programs (MW)



$P_{b m,t}^{Dem,(s/k)}$	Active demand after DSR program (MW)
$q_{m,t}^{Dem,k}$	Reactive demand after DSR program (MVar)
$S_{m,t}^{k,\uparrow}, S_{m,t}^{k,\downarrow}$	Slack variables of power curtailment (MW)
$\lambda_{m,t}^k, \mu_{m,t}^k$	Dual variables of power balance constrain of sub-problems
$F_{D,t}, \gamma_{D,t}$	Upper and lower bounds of DSOs' costs (\$)
$H_{m,n}^{t,k}, I_{m,n}^{t,k}$	Axillary variables for SOCP relaxation
<b>Constants</b>	
$C_{j,g}^{En}, C_{dg}^{En}$	Coefficient of production cost of generators and DGs (\$/MWh)
$C_b^{En}, C_m^{En}$	Coefficient of energy supplied by DSR programs (\$/MWh)
$C_g^{ST}, C_g^{SD}, C_g^{F\&C}$	Cost of start-up/shut-down (\$) and fixed cost of generators (\$/h)
$C_{(g/dg)}^{Re,(1/d)}$	Cost of reserve capacity provided by CGs and DGs (\$/MW)
$C_{(w/wd)}^{Re,(1/d)}$	Cost of reserve capacity provided by wind farms (\$/MW)
$C_{(b/m)}^{Re,(1/d)}$	Cost of reserve capacity provided by DSR programs (\$/MW)
$Ru_{(g/dg)}, Rd_{(g/dg)}$	Ramp rate limits of CGs and DGs (MW/h)
$P_l^{max}, S_{m,n}^{max}$	Flow limits of transmission (MW) and distribution lines (MVA)
$RS_g, RD_g$	Start-up/shut-down ramp rates of generators (MW/h)
$DB_m^D$	Connectivity matrix of buses to distribution system $D$
$GD_{dg}^D, DW_{wd}^D$	Connectivity matrix of DGs/wind farms to distribution system $D$
$X_l, S_{base}$	Reactance of transmission lines (p.u.) and base power (MW)
$P_{(w/wd),t}^{max,(s/k)}$	Forecasted values of absorbable power for wind farms at transmission/distribution system (MW)
$P_{(g/dg),t}^{(max/min)}$	Generation limits of generators and DGs (MW)
$Q_{dg,t}^{(max/min),k}$	Reactive generation limits of DGs (MVar)
$P_{(b/m),t}^{Dem,(s/k)}$	Active demands at transmission/distribution grids (MW)
$T_{g,(on/off)}^{min}$	Minimum online/offline duration of generators (h)
$\Gamma_{(b/m),t}$	Coefficient of demands' maximum allowed participation
$\pi_{t,s}, \pi_{t,k}^D$	Probability of scenarios in T&D systems
$Y_m^n, G_m^n, B_m^n$	Admittance, conductance, and susceptance of lines (p.u.)
$V_m^{min}, V_m^{max}$	Voltage magnitude limits of distribution buses (p.u.)

## ORCID

Mabdi Habibi  <https://orcid.org/0000-0002-5211-9201>

Vahid Vahidinasab  <https://orcid.org/0000-0002-0779-8727>

## REFERENCES

- Rossi, M., Migliavacca, G., Vigano, G., Siface, D., Madina, C., Gómez, I., et al.: TSO-DSO coordination to acquire services from distribution grids: Simulations, cost-benefit analysis and regulatory conclusions from the SmartNet project. *Electr. Power Syst. Res.* 189, 106700 (2020)
- Habibi, M., Vahidinasab, V., Pirayesh, A., Shafie-khah, M., Catalão, J.P.: An enhanced contingency-based model for joint energy and reserve markets operation by considering wind and energy storage systems. *IEEE Trans. Ind. Inf.* 17, 3241–3252 (2020)
- Habibi, M., Vahidinasab, V., Sepasian, M.S., Allahham, A., Giaouris, D., Taylor, P., et al.: Stochastic procurement of fast reserve services in renewable integrated power systems. *IEEE Access* 9, 30946–30959 (2021)
- Migliavacca, G.: TSO-DSO Interactions and Ancillary Services in Electricity Transmission and Distribution Networks: Modeling, Analysis and Case-Studies. Springer, New York (2019)
- Baltputnis, K., Repo, S., Mutanen, A.: The role of TSO-DSO coordination in flexibility asset prequalification. In: *2020 17th International Conference on the European Energy Market (EEM)*. Stockholm, Sweden, pp. 1–5 (2020)
- Nawaz, A., Wang, H., Wu, Q., Kumar Ochani, M.: TSO and DSO with large-scale distributed energy resources: A security constrained unit commitment coordinated solution. *Int. Trans. Electr. Energy Syst.* 30, e12233 (2020)
- E. DSO, & CEDEC, & ENTSO-E, & Euroelectric, & GEODE.: TSO-DSO Report-An Integrated Approach to Active System Management. [https://www.entsoe.eu/Documents/Publications/Positionpapersandreports/TSO-DSO\\_ASM\\_2019\\_190416.pdf](https://www.entsoe.eu/Documents/Publications/Positionpapersandreports/TSO-DSO_ASM_2019_190416.pdf) (accessed 20/01/2021)
- CEER Position Paper on the Future DSO and TSO Relationship. [https://www.ceer.eu/documents/104400/3731907/C16-DS-26-04-DSO-TSO-relationship\\_PP\\_21-Sep-2016.pdf](https://www.ceer.eu/documents/104400/3731907/C16-DS-26-04-DSO-TSO-relationship_PP_21-Sep-2016.pdf) (accessed: 24/01/2021)
- Gerard, H., Rivero, E., Six, D.: Basic schemes for TSO-DSO coordination and ancillary services provision. *SmartNet* 1, 12 (2016)
- Schittekatte, T., Meeus, L.: Flexibility markets: Q&A with project pioneers. *Util. Policy* 63, 101017 (2020)
- Antony, Z. & Helfried, B. : TSO-DSO interaction: an Overview of current interaction between transmission and distribution system operators and an assessment of their cooperation in Smart Grids (2014). [https://www.iea-iscan.org/wp-content/uploads/2014/02/ISGAN\\_DiscussionPaper\\_TSODSOInteractionOverview\\_2014.pdf](https://www.iea-iscan.org/wp-content/uploads/2014/02/ISGAN_DiscussionPaper_TSODSOInteractionOverview_2014.pdf) (accessed: 24/01/2021)
- Betancourt-Paulino, P., Chamorro, H.R., Soleimani, M., Gonzalez-Longatt, F., Sood, V.K., Martinez, W.: On the perspective of grid architecture model with high TSO-DSO interaction. *IET Energy Syst. Integr.* 3, 1–12 (2021)
- Givisiez, A.G., Petrou, K., Ochoa, L.F.: A review on TSO-DSO coordination models and solution techniques. *Electr. Power Syst. Res.* 189, 106659 (2020)
- Habibi, M., Vahidinasab, V., Sepasian, M.S.: Application of mobile energy storage to facilitate energy transfer between tso and dso networks. In: *2020 10th Smart Grid Conference (SGC)*. Kashan, Iran, pp. 1–3 (2020)
- Silva, J., Sumaili, J., Bessa, R.J., Seca, L., Matos, M.A., Miranda, V., et al.: Estimating the active and reactive power flexibility area at the TSO-DSO interface. *IEEE Trans. Power Syst.* 33, 4741–4750 (2018)
- Gonzalez, D.M., Hachenberger, J., Hinker, J., Rewald, F., Häger, U., Rehtanz, C., et al.: Determination of the time-dependent flexibility of active distribution networks to control their TSO-DSO interconnection power flow. In: *2018 Power Systems Computation Conference (PSCC)*. Dublin, Ireland, pp. 1–8 (2018)
- Edmunds, C., Galloway, S., Elders, I., Bukhsh, W., Telford, R.: Design of a DSO-TSO balancing market coordination scheme for decentralised energy. *IET Gener. Transm. Distrib.* 14, 707–718 (2019)
- Dzikowski, R.: DSO-TSO coordination of day-ahead operation planning with the use of distributed energy resources. *Energies* 13, 3559 (2020)
- Sun, W., Golshani, A.: Distributed restoration for integrated transmission and distribution systems with DERs. *IEEE Trans. Power Syst.* 34, 4964–4973 (2019)

20. Mohammadi, A., Mehrtash, M., Kargarian, A.: Diagonal quadratic approximation for decentralized collaborative TSO+ DSO optimal power flow. *IEEE Trans. Smart Grid* 10, 2358–2370 (2019)
21. Kargarian, A., Mehrtash, M., Falahati, B.: Decentralized implementation of unit commitment with analytical target cascading: A parallel approach. *IEEE Trans. Power Syst.* 33, 3981–3993 (2018)
22. Kargarian, A., Fu, Y.: System of systems based security-constrained unit commitment incorporating active distribution grids. *IEEE Trans. Power Syst.* 29, 2489–2498 (2014)
23. Li, Z., Guo, Q., Sun, H., Wang, J.: Coordinated economic dispatch of coupled transmission and distribution systems using heterogeneous decomposition. *IEEE Trans. Power Syst.* 31, 4817–4830 (2016)
24. Tang, K., Dong, S., Cui, J., Li, Y., Song, Y.: Synthesised-objective collaborative model and its solution algorithm for transmission–distribution coordinated optimisation. *IET Gener. Transm. Distrib.* 14, 752–761 (2019)
25. Tang, K., Dong, S., Ma, X., Fei, Y., Song, Y.: Heterogeneous-decomposition-based coordinated optimisation for integrated transmission and distribution networks considering communication conditions. *IET Gener. Transm. Distrib.* 14, 2558–2565 (2020)
26. Xue, Y., Li, Z., Lin, C., Guo, Q., Sun, H.: Coordinated dispatch of integrated electric and district heating systems using heterogeneous decomposition. *IEEE Trans. Sustainable Energy* 11, 1495–1507 (2020)
27. Lin, C., Wu, W., Zhang, B., Wang, B., Zheng, W., Li, Z.: Decentralized reactive power optimization method for transmission and distribution networks accommodating large-scale DG integration. *IEEE Trans. Sustainable Energy* 8, 363–373 (2017)
28. Yuan, Z., Hesamzadeh, M.R.: Hierarchical coordination of TSO-DSO economic dispatch considering large-scale integration of distributed energy resources. *Appl. Energy* 195, 600–615 (2017)
29. Gonzalez, D.M., Myrzik, J., Rehtanz, C.: The smart power cell concept: Mastering TSO–DSO interactions for the secure and efficient operation of future power systems. *IET Gener. Transm. Distrib.* 14, 2407–2418 (2020)
30. Stock, D.S., Sala, F., Berizzi, A., Hofmann, L.: Optimal control of wind farms for coordinated TSO-DSO reactive power management. *Energies* 11, 173 (2018)
31. Retorta, F., Aguiar, J., Rezende, I., Villar, J., Silva, B.: Local market for TSO and DSO reactive power provision using DSO grid resources. *Energies* 13, 3442 (2020)
32. Bobo, L., Venzke, A., Chatzivasileiadis, S.: Second-order cone relaxations of the optimal power flow for active distribution grids: Comparison of methods. *Int. J. Electr. Power Energy Syst.* 127, 106625 (2021)
33. Engelbrecht, D., Matthes, U., Junghans, M., Knobloch, A., Dorendorf, S., Evers, T., et al.: Balancing control and congestion management with increasing decentralized generation-possible solutions based on TSO-DSO cooperation. In: *International ETG Congress 2017*. Bonn, pp. 1–8 (2017)
34. Habibi, M., Vahidinasab, V., Aghaei, J., Mohammadi-Ivatloo, B.: Assessment of energy storage systems as a reserve provider in stochastic network constrained unit commitment. *IET Smart Grid* 4, 139–150 (2021)
35. Papalexopoulos, A., Frowd, R., Birbas, A.: On the development of organized nodal local energy markets and a framework for the TSO-DSO coordination. *Electr. Power Syst. Res.* 189, 106810 (2020)
36. Habibi, M., Vahidinasab, V., Shafie-khah, M., Catalão, J.P.: Coordinated scheduling of energy storage systems as a fast reserve provider. *Int. J. Electr. Power Energy Syst.* 130, 106941 (2021)
37. Jabr, R.A.: Radial distribution load flow using conic programming. *IEEE Trans. Power Syst.* 21, 1458–1459 (2006)
38. Benders, J.F.: Partitioning procedures for solving mixed-variables programming problems. *Numer. Math.* 4, 238–252 (1962).
39. Shahidehpour, M., Yamin, H., Li, Z., *Market Operations in Electric Power Systems: Forecasting, Scheduling, and Risk Management*. John Wiley & Sons, Hoboken, NJ (2003)
40. Habibi, M. & Vahidinasab, V. : TD-RTS24. <http://www.vahidinasab.com/data/JNL/TD-RTS24.xlsx> (accessed: 10/08/2021)

**How to cite this article:** Habibi, M., Vahidinasab, V., Sepasian, M.S.: A privacy-preserving approach to day-ahead TSO-DSO coordinated stochastic scheduling for energy and reserve. *IET Gener. Transm. Distrib.* 16,163–180 (2022).

<https://doi.org/10.1049/gtd2.12286>

**APPENDIX A: INPUT DATA OF STOCHASTIC PARAMETERS**

See Figures A1 and A2.

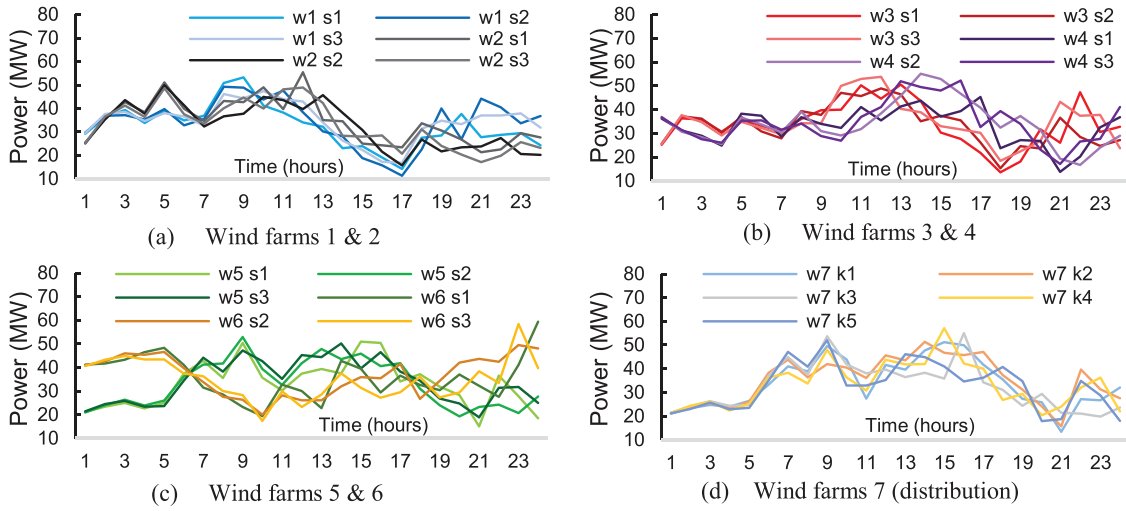


**FIGURE A1** Scenarios of available wind power

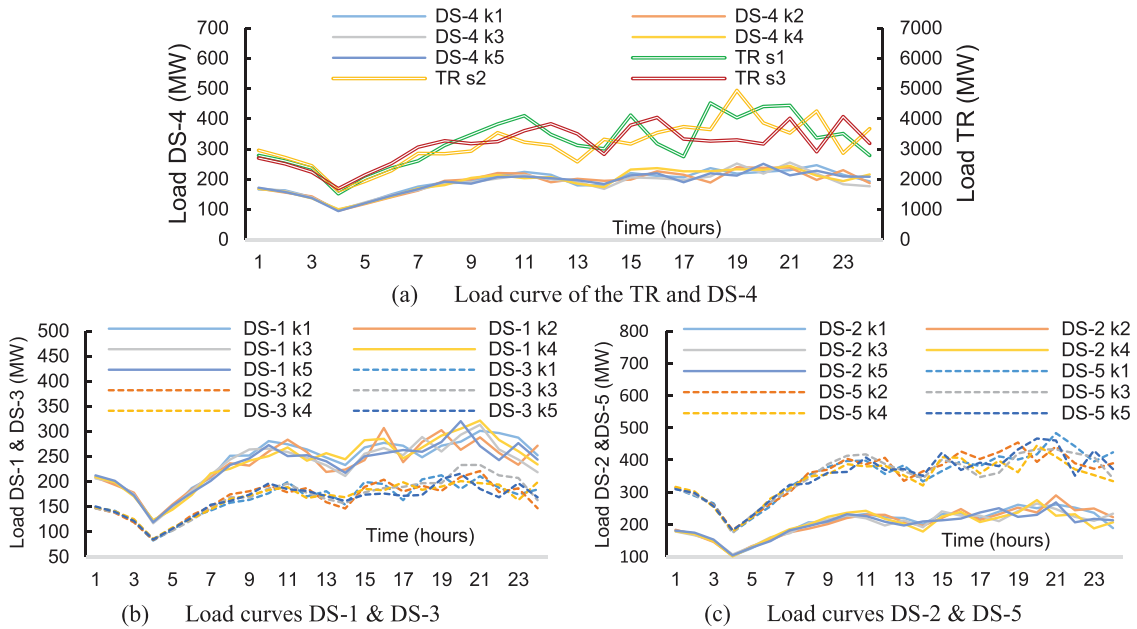


**FIGURE A2** Data of load curves at transmission and distribution systems